

1 A New Approach for Quantifying Epithelial and Stromal Thickness
2 Changes after Orthokeratology Contact Lens Wear

3 Ziyang Ran^{1*}, Joshua Moore^{1,2}, Fan Jiang³, Hongmei Guo⁴, Ashkan Eliasy¹,
4 Bernardo T Lopes^{1,5}, FangJun Bao³, Jun Jiang^{3*},
5 Ahmed Abass^{1,6}, Ahmed Elsheikh^{1,7,8}

6
7 ¹ School of Engineering, University of Liverpool, Liverpool, UK

8 ² Department of Mathematical Sciences, School of Physical Sciences, University of
9 Liverpool, Liverpool, UK

10 ³ Eye Hospital, Wenzhou Medical University, Wenzhou, China

11 ⁴ College of Biomedical Engineering, Taiyuan University of Technology, Taiyuan City,
12 Shanxi Province, China

13 ⁵ Federal University of São Paulo, 1500 Vila Clementino, São Paulo, 04021-001, Brazil

14 ⁶ Department of Production Engineering and Mechanical Design, Faculty of
15 Engineering, Port Said University, Egypt

16 ⁷ Beijing Advanced Innovation Centre for Biomedical Engineering, Beihang University,
17 Beijing, China

18 ⁸ National Institute for Health Research (NIHR) Biomedical Research Centre at
19 Moorfields Eye Hospital NHS Foundation Trust and UCL Institute of Ophthalmology,
20 London, UK

21
22 ***Author for correspondence:**

23 Ziyang Ran, School of Engineering, University of Liverpool, Liverpool, L69 3GH, UK.

24 Z.Ran@liverpool.ac.uk

25 Jun Jiang, Eye Hospital, Wenzhou Medical University, Wenzhou, 325027, China.

26 jjhsj@hotmail.com

27
28 **Keywords:** eye; cornea; OCT; orthokeratology; contact lenses; epithelium

29
30 **Number of words:** 5634

31 **Abstract**

32 **Purpose:** To develop an automatic segmentation approach of optical coherence
33 tomography (OCT) images and to investigate the changes in epithelial and stromal
34 thickness profile and radius of curvature after the use of orthokeratology (Ortho-K)
35 contact lenses.

36 **Methods:** A total of 45 right eyes from 52 participants were monitored before, and
37 after one month of, uninterrupted over-night Ortho-K lens wear. The tomography of
38 their right eyes was obtained using optical OCT and rotating Scheimpflug imaging
39 (OCULUS Pentacam). A custom-built MATLAB code for automatic segmentation of
40 corneal OCT images was created and used to assess changes in epithelial thickness,
41 stromal thickness, corneal and stromal profiles and radii of curvature before, and after
42 one month of , uninterrupted over-night wear of Ortho-K lenses.

43 **Results:** In the central area (0-2 mm diameter), the epithelium thinned by 12.8 ± 6.0
44 μm (23.8% on average, $p < 0.01$) after one month of Ortho-K lens wear. In the
45 paracentral area (2–5 mm diameter), the epithelium thinned nasally and temporally
46 (by 2.4 ± 5.9 μm , 4.5% on average, $p = 0.031$). The stroma thickness increased in the
47 central area (by 4.8 ± 16.1 μm , $p = 0.005$). The radius of curvature of the central corneal
48 anterior surface increased by 0.24 ± 0.26 mm (3.1%, $p < 0.01$) along the horizontal
49 meridian and by 0.34 ± 0.18 mm (4.2%, $p < 0.01$) along the vertical meridian. There
50 were no significant changes in the anterior and posterior stromal radius of curvature.

51 **Conclusions:** This study introduced a new method to automatically detect the anterior
52 corneal surface, the epithelial posterior surface, and the posterior corneal surface in
53 OCT scans. Overnight wear of Ortho-K lenses caused thinning of the central corneal
54 epithelium. The anterior corneal surface became flatter while the anterior and
55 posterior surfaces of the stroma did not undergo significant changes. The results are
56 consistent with the changes reported in previous studies. The reduction in myopic
57 refractive error caused by Ortho-K lens wear was mainly due to changes in corneal
58 epithelium thickness profile.

59 Introduction

60 The prevalence of myopia has increased rapidly in recent years. In 2010, there were
61 1950 million people with myopia globally, and the number is expected to increase to
62 4758 million, or 49.8% of the population, by 2050 ⁽¹⁾. Orthokeratology (Ortho-K) is a
63 clinical technique that temporarily reshapes the cornea to eliminate or reduce the
64 refractive error ⁽²⁾. Ortho-K lenses are commonly worn during sleep and removed
65 immediately after waking up, allowing clear unaided vision in daytime. The lenses are
66 made of rigid gas permeable (RGP) material and seek to reduce myopia by corneal
67 flattening ⁽³⁾. The base curve of the lens is flatter than the central corneal radius of
68 curvature and the secondary curve (in the paracentral region) is steeper than the base
69 curve ⁽⁴⁾. Earlier studies showed that Ortho-K contact lenses effectively reduce myopia,
70 providing reliable refractive correction up to 4.5 D ^(5, 6). High myopia has been partially
71 reduced by Ortho-K lenses in some studies ^(7, 8). Yet, despite interest in Ortho-K lenses,
72 the mechanism by which they interact with the cornea is still not fully understood. In
73 several studies, epithelial thickness changes were recognized as the main cause of
74 corneal reshaping ⁽⁹⁻¹⁶⁾.

75 Various methods have been used to measure the geometrical changes that take place
76 in the cornea as a result of wearing Ortho-K lenses, and in particular the thickness
77 changes in the stroma and epithelium, and the radius of curvature changes in the
78 cornea's anterior and posterior surfaces. The rotating Scheimpflug camera provides
79 reliable 3D, non-contact imaging of corneal tomography ⁽¹⁷⁾, and has good
80 reproducibility and repeatability in measuring radii of curvature and thickness in both
81 normal and keratoconic eyes ⁽¹⁸⁾. Using Scheimpflug imaging (the Pentacam HR
82 system), Gonzalez-Mesa et al. reported significant reductions in anterior chamber
83 depth and flattening in the posterior corneal surface in 34 subjects after one year of
84 wearing Ortho-K lenses ⁽¹⁹⁾. Anterior segment optical coherence tomography (OCT)
85 was also used to measure stromal and epithelial thickness profiles ⁽²⁰⁻²²⁾ with higher
86 scanning speed and better resolution relative to Scheimpflug systems ^(21, 22). With OCT,
87 Neito-Bona et al. measured the epithelial thickness in 27 subjects before and one
88 month after wearing Ortho-K lenses, and showed significant epithelial thickness
89 reductions in the central cornea up to 2 mm diameter ⁽²³⁾. Similar observations, and
90 also epithelial thickening in the peripheral region, were made based on analysis of
91 OCT corneal scans ^(11, 15, 16, 24).

92 Different methods to detect epithelial and stromal surfaces in OCT images were
93 reported in the literature. Elsayy et al. used Randomized Hough Transform to develop
94 an OCT image segmentation algorithm, including estimations of corneal thickness ⁽²⁵⁾.
95 The resulting automatic segmentation of 15 corneal OCT images was compared with
96 manual segmentation by two trained operators, and the mean difference between the
97 automated and manual methods was $5.66 \pm 6.38 \mu\text{m}$. Eichel et al. detected the anterior
98 and posterior surfaces of the cornea automatically using the difference in refractive
99 index between the cornea and both the air and aqueous, and used a low-dimensional
100 function to describe the cornea's three inner layers ⁽²⁶⁾. Elsayy et al. also detected the
101 cornea's outer surfaces and transformed them into a flat form to locate the inner layers
102 ⁽²⁵⁾. Compared with manual segmentation, this method has better repeatability and
103 similar precision.

104 While these methods were largely successful in tracing the anterior and posterior
105 surfaces, difficulties remained in detecting the inner surfaces, and some methods
106 involved manual segmentation steps. These points were the drivers to develop a new
107 automatic segmentation method in this study that can detect with high repeatability
108 both outer and inner corneal surfaces.

109

110 **Materials and Methods**

111 ***Study participants***

112 This prospective study included 52 participants who were prescribed Ortho-K lenses
113 for myopia correction in the Eye Hospital of Wenzhou Medical University between
114 December 2016 and August 2019. The inclusion criteria included age between 8 and
115 18 years, best corrected visual acuity (BCVA) greater than 20/25, spherical equivalent
116 between -1.00 D and -6.00 D, and intraocular pressure between 11 and 21mmHg.
117 Participants with history of Ortho-K lens wear, contact lens contra-indications, related
118 eye systemic diseases, uncorrected visual acuity below 20/25, or unacceptable lens
119 decentration (over 1mm) after regular wear were excluded. These inclusion and
120 exclusion criteria, along with details of the clinical care adopted, follow those presented
121 in our earlier clinical study⁽²⁷⁾. The study was approved by the Ethics Committee of the
122 eye hospital and complied with the Declaration of Helsinki. Examinations were only

123 conducted after the subjects and their guardians had fully understood and signed
124 informed consent.

125 ***Lens fitting***

126 Participants were fitted with orthokeratology lenses produced by Euclid Systems Corp.,
127 USA, Paragon CRT, USA and Dreamlite, Germany. The Euclid lenses, manufactured
128 with Boston Equalens II material, had Dk of $85 \times 10^{-11}(\text{cm}^2/\text{sec})$ ($\text{mLO}_2/\text{mL} \times \text{mmHg}$),
129 while the Paragon CRT lenses were made of Paragon HDS 100 Paflucocon D material
130 with Dk of $100 \times 10^{-11}(\text{cm}^2/\text{sec})$ ($\text{mLO}_2/\text{mL} \times \text{mmHg}$). Finally, the Dreamlite lenses
131 were manufactured with the Boston XO hexafocon-A material that had
132 Dk of $100 \times 10^{-11}(\text{cm}^2/\text{sec})(\text{mLO}_2/\text{mL} \times \text{mmHg})$. The lenses were fitted to both eyes by
133 an experienced clinician (JJ) according to the manufacturer's guidelines, and
134 participants were requested to wear the lenses for eight hours each night except in
135 cases of illness or abnormal ocular symptoms^(27, 28).

136 ***OCT and Pentacam***

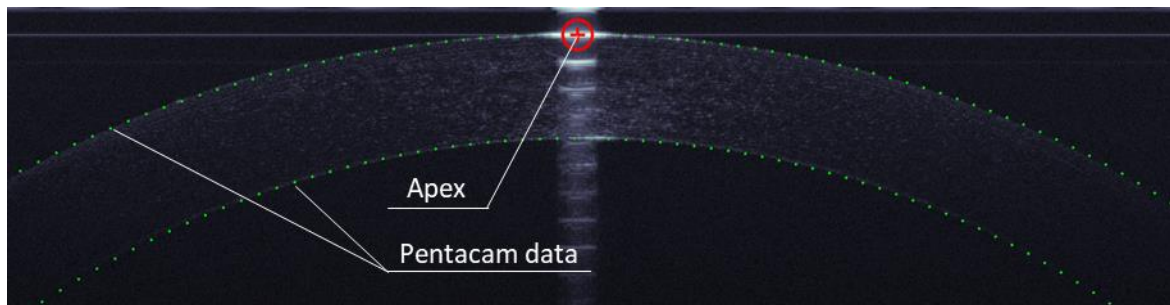
137 A custom-built ultra-high-resolution, spectral-domain OCT (UHR-SD-OCT) with 3 μm
138 axial resolution, mounted on a standard slit-lamp, was used to measure corneal
139 tomography. The OCT acquired images with 24k A-lines per second, and each B-scan
140 included 2048×1365 pixels, corresponding to a scan width of 8.93 mm in the air and
141 a scan depth of 2.00 mm. Corneal profiles were then created from scans of the vertical
142 and horizontal meridians. A Pentacam HR (Oculus, Wetzlar, Germany) with a
143 Scheimpflug camera was used to scan the anterior segment of all eyes included in the
144 study.

145 All OCT and Pentacam HR measurements were performed by an experienced
146 operator (FJ) at baseline and after one-month of Ortho-K lens wear. The
147 measurements were taken between 9 AM and 11 AM to minimise the diurnal variation.
148 The measurements were repeated until an examination quality of "OK" was obtained^{(27,}
149 ²⁸⁾.

150 After reviewing the medical records of the right eyes of the 52 study participants, seven
151 were excluded because of the blurriness of OCT images, which resulted in failure to
152 locate the epithelial surface. Therefore, a total of 45 eyes were included in the analysis.

153 ***Data Processing***

154 Apex detection: Each B-scan OCT image included 2048×1365 pixels, where the
 155 brightness of each pixel varied from 0 to 256. The cornea's apex was detected first for
 156 being the brightest region in both horizontal and vertical scans, Figure 1. The centre
 157 of this region was set as the origin point of a Cartesian coordinate system with the
 158 patient's eye in the negative Z-direction. The nasal-temporal direction was assigned
 159 to the X-axis in horizontal scans, while the inferior-superior direction was assigned to
 160 the Y-axis in vertical scans.



161
 162 *Figure 1 Apex detection (red cross and circle) and the Pentacam's elevation data (green*
 163 *dots) for the same corneal outer surfaces*

164 Exclusion of data that is likely to be outside cornea: A binary weighting function based
 165 on the bi-conic model (Equation 1) was introduced to eliminate data above the upper
 166 boundary curve. The model was created by a binary weighting function and used to
 167 extend a circular equation by adding an asphericity coefficient, Q_u , to control the radius
 168 of curvature of the front boundary. A tolerance T_u (with a value of 0.01 mm, which was
 169 found adequate in our preliminary study's trials) was added to the equation to shift the
 170 weighting function boundary slightly above the corneal anterior surface.

171
$$Z_u = T_u + \frac{\sqrt{R_u^2 - X_u^2(Q_u+1)} - R_f}{Q_u+1} \quad \text{Equation 1}$$

172 The asphericity factor Q_u is synonymous with the front boundary's radius of curvature,
 173 with positive values leading to increasing steepness away from the centre point, and
 174 negative values inducing a flattening effect. In this boundary, Q_u was set to -0.2^(29, 30)
 175 based on initial trials of the method. The parameter R_u is the radius of the upper
 176 boundary, set to 10 mm to be considerably bigger than the cornea's range of anterior
 177 surface radius^(29, 30) to avoid any possibility of interference with that surface.

178 Similarly, a lower boundary was constructed with the similar conic model presented in
 179 Equation 2. The tolerance T_l , set to -0.8 mm – substantially bigger in magnitude than

180 normal values of corneal thickness ⁽³¹⁾, was used to avoid conflict with the corneal
181 posterior surface. Meanwhile, the lower boundary curve radius, R_l , was set to 5 mm
182 with an asphericity coefficient Q_l set to -0.1 – both values were found adequate in the
183 study's initial trials. This choice of parameters avoided intersection between the
184 boundary surfaces and the cornea's cross-section, while removing most of the
185 unwanted portions of the image.

$$186 \quad Z_l = T_l + \frac{\sqrt{R_l^2 - X_l^2(Q_l+1)} - R_l}{Q_l+1} \quad \text{Equation 2}$$

187 Auto-detection of corneal surfaces: To reduce processing time, 129 evenly spaced Z-
188 lines, parallel to the Z-axis, were considered including one aligned with the origin point
189 of the Cartesian system. Surface detection was performed on only these lines.

190 Topography measurements of the corneal anterior surface along the principal vertical
191 and horizontal meridians taken for the same corneas using the Pentacam (Oculus,
192 Germany) (Figure 1) were fitted to a 5th order polynomial. This polynomial order was
193 sufficient to keep the root mean square of error of fit with the topography data below
194 2.5 μm , while avoiding overfitting. The polynomial was used to derive two profiles of
195 the anterior surface along the vertical and horizontal meridians, and search was then
196 conducted to locate the point with the highest brightness along each of the 129 Z-lines
197 that was within $\pm 10 \mu\text{m}$ above or below the relevant profile. The resulting 129 points
198 were fitted to a 5th order polynomial, and points that were away from the polynomial
199 by 7 μm were considered outliers and were excluded before fitting the remaining points
200 to another 5th order polynomial. This exercise was repeated until no outliers were
201 identified, and this process was then repeated for the posterior surface.

202 Epithelium posterior surface detection: At least 5 points on the epithelium posterior
203 surface were manually selected by the operator, including a point at each end of the
204 visible width of the epithelium surface, and three points spaced roughly-equally in
205 between. These five points were fitted to a lower (4th) order polynomial to form an
206 epithelium base curve, while avoiding overfitting. Points along the same 129 Z-lines
207 (but only those lines between the endpoints marked above), that had the highest
208 brightness and were within 10 μm from the base curve, were identified and assumed
209 to be on the epithelial posterior surface. These points were fitted to a 5th order
210 polynomial, and a process was followed to exclude points that were farther from the

211 fitting curve by more than 7 μm . Fitting of the remaining points to a new polynomial
212 and excluding the far points were repeated until no points could be excluded. The
213 remaining points were then saved and used to represent the epithelial posterior
214 surface.

215 Results confirmation: The lines representing the corneal anterior surface, corneal
216 posterior surface and epithelium posterior surface were displayed on the OCT image
217 to enable a visual check of all the fitting processes before accepting the results or
218 repeating parts of the analysis which produced unsatisfactory results.

219 The epithelial thickness profiles in the horizontal and vertical scans were then adjusted
220 proportionally to give the same thickness at the two central points ($X = 0 \text{ mm}$), and the
221 same process was followed for the stromal thickness profiles.

222 Once these steps were completed, the thickness profiles of both the stroma and
223 epithelium were used to determine the radius of curvature profile along the three outer
224 and inner surfaces in each scan, Figure 2.

225

226 **Data Analysis**

227 Data were recorded and analysed in MATLAB (version 2020a for windows). All data
228 was tested with the Kolmogorov-Smirnov normality test. Quantitative variables were
229 expressed as mean \pm standard deviation. Comparisons between pre-Ortho-K lens

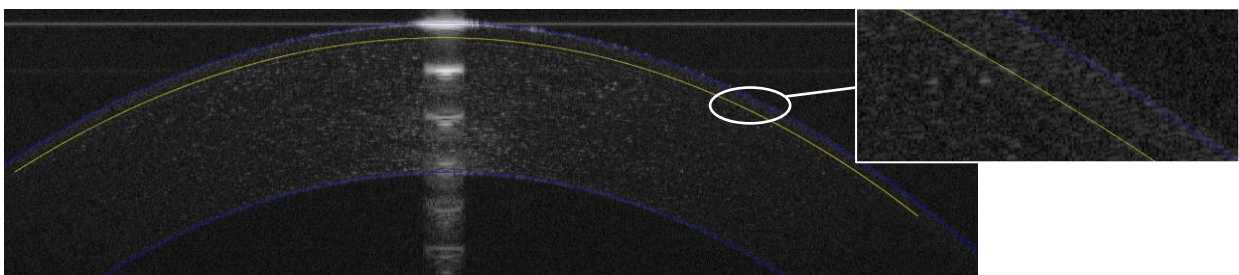
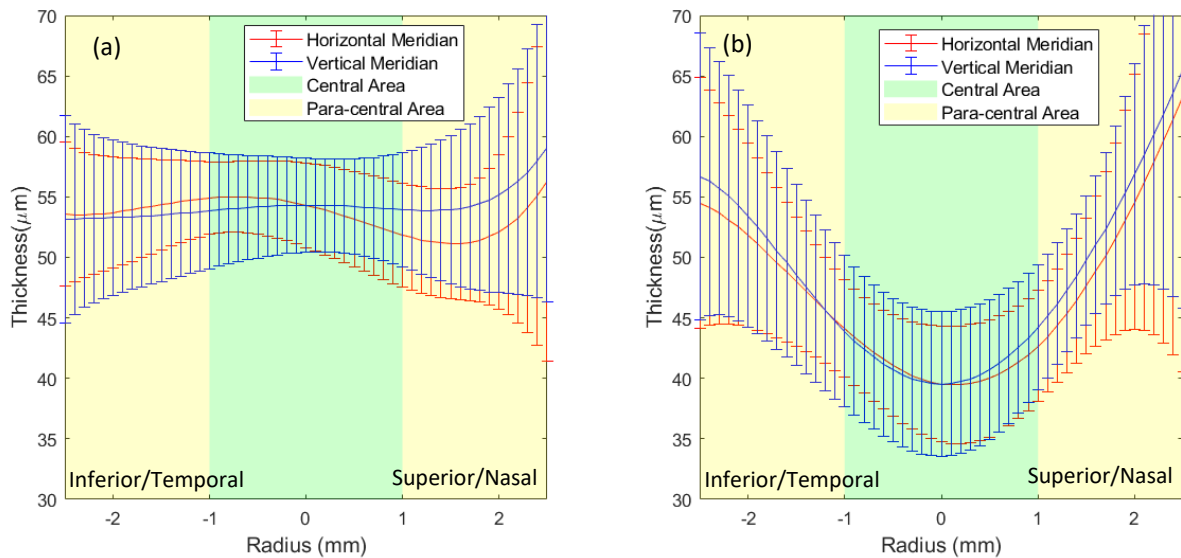


Figure 2 automated segmentation result of corneal anterior, posterior, and epithelial interfaces

230 wear and post-Ortho-K lens wear were performed using the Paired t-test. Statistical
231 significance was defined as $p < 0.05$.

232 **Results**



233 *Figure 3 Mean epithelial thickness (a) before and (b) after Ortho-K lens wear*

234 This study focused on the corneal area within 5mm diameter because of the limitation
 235 in visible width of the epithelial surface on OCT images.

236 The thickness changes in the epithelium, stroma and the whole cornea were evaluated
 237 within the central area (0 – 2 mm diameter) and the paracentral area (2 – 5 mm
 238 diameter) in Tables 1 and 2, Figures 3 and 4. Overall, the epithelial thickness
 239 decreased by $12.8 \pm 6.0 \mu\text{m}$ (23.8% on average, $p < 0.01$) in the central area, which
 240 was larger than the thickness changes in the paracentral area (decreased $2.4 \pm 5.9 \mu\text{m}$,
 241 4.5% on average, $p = 0.031$ along the horizontal meridian and increased $2.2 \pm 7.1 \mu\text{m}$,
 242 4.2% on average, $p = 0.086$ along the vertical meridian). In the central area, the
 243 epithelium experienced thinning of up to $14.8 \mu\text{m}$ at the centre in the vertical scans (p
 244 < 0.01 , Figure 4), and up to $15.0 \mu\text{m}$ at -0.2mm away from the centre in the horizontal
 245 scans ($p < 0.01$, Figure 4). The significance of the thickness changes was close to 0
 246 in the area from $X = -1.5 \text{ mm}$ to $X = 1.5 \text{ mm}$ in both meridians, then the changes
 247 became insignificant from a radius of 1.7 mm onwards.

248 For the stroma, the thickness increased moderately in both the central and paracentral
 249 areas. The thickness increase was $4.8 \pm 16.1 \mu\text{m}$ ($p < 0.01$) in the central area, while in
 250 the paracentral area, the increase was $3.6 \pm 20.0 \mu\text{m}$ ($p = 0.272$) along the vertical
 251 meridian, and $2.4 \pm 17.2 \mu\text{m}$ ($p = 0.418$) along the horizontal meridian. In these results,
 252 the mean changes in stromal thickness were smaller than corresponding changes in

253 epithelial thickness ($p < 0.05$), while the standard deviation values in the epithelium
 254 were significantly smaller than in the stroma ($12.8 \pm 6.0 \mu\text{m}$ vs $4.8 \pm 16.1 \mu\text{m}$, $p < 0.01$),
 255 indicating much more consistent changes in epithelial thickness. The stromal
 256 thickness changes were significant at $X = -0.5\text{mm}$ to $X = 0 \text{ mm}$ in the horizontal
 257 meridian (all $p < 0.05$), elsewhere the changes were not significant.

258 The overall thickness changes in the whole cornea indicated similar trends in the
 259 horizontal and vertical scans, including a decrease in the central area and an increase
 260 near the edges of the paracentral area. The cornea thinned within the central area by
 261 up to $11.9 \mu\text{m}$ horizontally ($p < 0.01$, Figure 4) and up to $12.2 \mu\text{m}$ vertically ($p < 0.01$,
 262 Figure 4). These changes were dominated by the thickness changes observed in the
 263 epithelium, which accounted for more than 60% of the total corneal thickness changes.

264 The central radius of curvature of the cornea's three surfaces before and after wearing
 265 Ortho-K lenses are compared in Table 3. The anterior surface experienced a
 266 significant increase in central radius (indicating a flattened anterior surface) after lens
 267 wear in both horizontal and vertical scans - the radius increase was $0.24 \pm 0.26 \text{ mm}$
 268 (3.1% , $p < 0.01$) along the horizontal meridian and $0.34 \pm 0.18 \text{ mm}$ (4.2% , $p < 0.01$)
 269 along the vertical meridian. In contrast, the epithelium posterior surface and the
 270 stromal posterior surface experienced slight and non-significant changes in the central
 271 radius of curvature after lens wear.

272 *Table 1 Average epithelial, stromal and corneal thickness in central area (0 - 2mm diameter)*

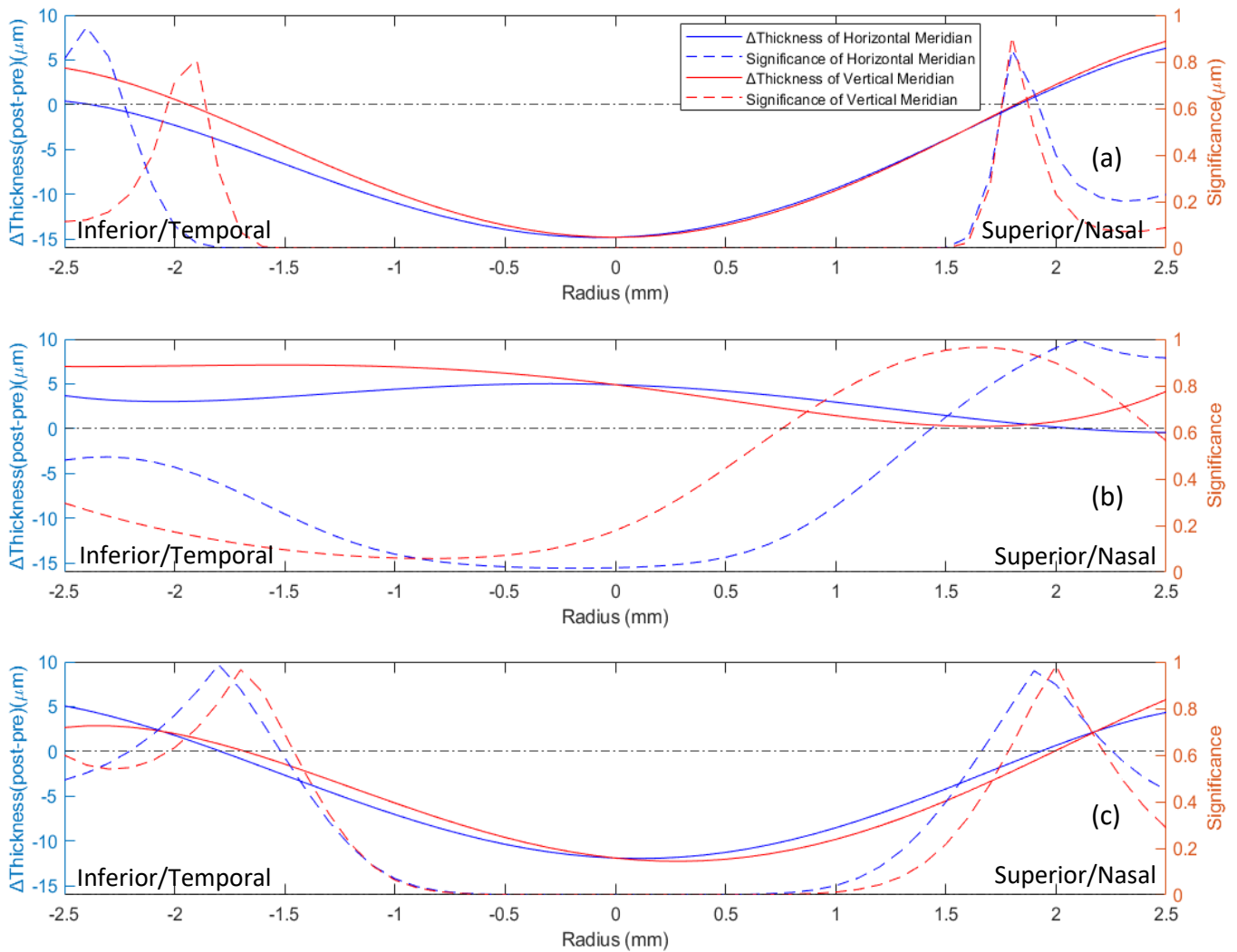
Mean \pm SD $/(\mu\text{m})$	Before Ortho-K lens wear	After Ortho-K lens wear	p-Value
Epithelium	53.6 ± 4.2	40.8 ± 5.3	$< 0.01^a$
Stroma	515.7 ± 28.1	520.5 ± 27.6	$< 0.01^a$
Cornea	569.3 ± 28.8	561.3 ± 28.8	$< 0.01^a$

273 ^a for Paired t-test $p < 0.01$

274 *Table 2 Average epithelial, stromal and corneal thickness in paracentral area (2 - 5mm*
 275 *diameter)*

Mean \pm SD $/(\mu\text{m})$	Before Ortho-K lens wear		After Ortho-K lens wear		p-Value	
	Horizontal meridian	Vertical meridian	Horizontal meridian	Vertical meridian	Horizontal meridian	Vertical meridian
Epithelium	52.6 ± 4.3	51.6 ± 6.0	50.2 ± 4.9	53.9 ± 6.1	0.031	0.086
Stroma	564.4 ± 29.9	565.5 ± 33.2	566.8 ± 28.5	569.1 ± 30.9	0.418	0.272
Cornea	618.6 ± 32.0	625.9 ± 35.4	617.9 ± 29.8	624.8 ± 27.0	0.848	0.767

276
 277
 278



280 *Figure 4 Values and significance of changes in thickness of (a) the epithelium, (b)*
 281 *the stroma, and (c) the whole cornea*

282 *Table 3 Central radius of curvature in OCT images, before and after orthokeratology*
 283 *lens wear.*

Mean ± SD/(mm)	Before Ortho-K lens wear		After Ortho-K lens wear		p-Value	
	Horizontal meridian	Vertical meridian	Horizontal meridian	Vertical meridian	Horizontal meridian	Vertical meridian
Corneal anterior surface	7.86 ± 0.27	7.60 ± 0.27	8.10 ± 0.21	7.94 ± 0.28	<0.01 ^a	<0.01 ^a
Epithelium posterior surface	7.95 ± 0.31	7.58 ± 0.28	7.90 ± 0.29	7.57 ± 0.35	0.211	0.718
Stromal posterior surface	6.50 ± 0.19	6.16 ± 0.24	6.51 ± 0.24	6.11 ± 0.24	0.780	0.139

284 ^a for Paired t-test p<0.01

285

286 **Discussion**

287 In this study, we used ocular anterior segment imaging by the OCT to determine the
288 thickness of the epithelium, the stroma and the total cornea in Ortho-K lens wearers
289 before, and after one month of, overnight lens wear. The measurements were taken
290 across the centre of the cornea along both the horizontal and vertical meridians. The
291 OCT image analysis indicated a significant reduction in central epithelial thickness by
292 $14.8 \pm 5.9 \mu\text{m}$ (or 26% of initial thickness) attributable to Ortho-K treatment ($p < 0.01$).
293 These results are consistent with earlier reports in which the central epithelial
294 thickness decreased over 30 days of lens wear by $15.8 \pm 3.3 \mu\text{m}$ in 18 eyes⁽¹²⁾, and by
295 to $18 \mu\text{m}$ in one eye⁽³²⁾. Other studies reported epithelium thickness reduction after
296 one week of lens wear of $10.6 \pm 4.2 \mu\text{m}$ ⁽¹⁰⁾, and $6.1 \pm 1.6 \mu\text{m}$ ⁽¹⁵⁾. Others adopted a one
297 day follow up and reported epithelial thickness reductions of $4.6 \pm 2.7 \mu\text{m}$ ⁽¹⁰⁾, and
298 $8.7 \pm 4.8 \mu\text{m}$ ⁽¹²⁾.

299 In contrast, the epithelial thickness increased in the paracentral area following Ortho-
300 K lens wear, but the increases were significantly lower than the decreases observed
301 in the central area. The thickness increases in the paracentral area could be due to
302 the deformation of epithelial cells caused by the negative pressure exerted by the
303 Ortho-K lens in the reverse curve zone^(23, 33), and remodelling of the epithelium due to
304 interference by the contact pressure with the normal centripetal migration of epithelial
305 cells from the limbus could be another reason. The paracentral thickness increases
306 observed in our study are compatible with the mean values reported by Zhang et al⁽¹⁵⁾,
307 in which epithelial thickness increases were noted in both the paracentral and
308 peripheral areas, albeit the change did not reach statistical significance. However,
309 Zhang also mentioned that the lack of significance of changes in the paracentral area
310 may have been due to variations in the size and location of reshaping areas among
311 individuals.

312 The present study also noted different epithelial thickness changes along the
313 horizontal and vertical meridians. Along the horizontal meridian, the point with the
314 largest thinning was 0.2 mm temporally away from the centre, while it was at the centre
315 in vertical scans. In the paracentral area, the epithelium thickened less on the temporal
316 side than on the nasal side, while the thickness changed evenly in vertical meridians.
317 As Lian et al⁽¹¹⁾ has explained, these differences may be due to variations in the eyelid
318 pressure acting in different eye regions. They could also be due to different lens-on-
319 eye decentrations among individuals⁽¹⁵⁾.

320 Stromal thickness experienced small, but significant, increases in the central area with
321 a large scatter in values. These findings are compatible with Reinstein's results ⁽³²⁾, in
322 which the stromal thickness was 5 µm larger, on average, after orthokeratology within
323 the central 3-mm diameter area. In the paracentral area, the stromal thickness
324 experienced only small and non-significant variations after lens wear. These results
325 are similar, to some extent, to a report by Nieto-Bona et al.⁽²³⁾ of central stromal
326 thinning and thickening in paracentral area after one month of lens wear although
327 these did not reach statistical significance, and another by Alharbi and Swarbrick
328 showing stromal thickness increases in the paracentral area over three months of lens
329 wear ⁽¹²⁾. While oedema by overnight hypoxia is a likely reason for central thickening,
330 paracentral thickness changes could be due to the combined effect of oedema and
331 the negative pressure in the reverse curve zone, as noted by Kim et al. ⁽¹⁶⁾. Overall,
332 the mechanism behind stromal thickness change is still unclear, and further work is
333 necessary to understand the effect of Ortho-K lens wear. However, the relatively small
334 changes in stromal thickness mean that the trends observed in overall corneal
335 thickness were dominated by the epithelial thickness changes. This finding agrees
336 with those reported by Zhang et al⁽¹⁵⁾, and Lian et al⁽¹¹⁾.

337 Our study also presented evidence that the corneal anterior surface experienced
338 significant flattening in the central region after Ortho-K lens wear. Aligned with the
339 results of this study, Maseedupally et al.⁽³⁴⁾ found that, after 14 days of Ortho-K lens
340 wear, the cornea became significantly flattened, and this flattening was greater on the
341 temporal side than the nasal side. Another study by Queiros et al.⁽³⁵⁾ reported central
342 anterior surface flattening of 3.16 ± 1.78 D after 12 months of lens wear, and similar
343 results were reported in Chen et al's study⁽¹⁰⁾. However, limited research was
344 conducted to study posterior corneal radii of curvature. Yoon et al. reported no
345 significant changes in either posterior corneal apical radius or asphericity after 14 days
346 of lens wear ⁽³⁶⁾. In our study, the central epithelial posterior surface and the stromal
347 posterior surface showed no significant radii of curvature changes after Ortho-K lens
348 wear. These results demonstrated that the Ortho-K lens mainly affected the epithelium
349 and the corneal anterior surface, a result that is in agreement with previously published
350 data ^(35, 37).

351 In this study, we established a method to automatically detect the three external and
352 internal corneal surfaces in OCT scans. The surface detection results for 45 patients

353 (180 OCT images) indicated the suitability of this method in segmenting corneal
354 images. The method builds on the success of previous work^(25, 38, 39), and provides
355 advantages in automation and validation in a relatively large patient population. To
356 further enhance the new method, denoising of original OCT images and auto-detection
357 of other corneal interfaces should be considered in future work.

358 This study has a number of limitations. First, the peripheral region of the cornea could
359 not be examined as most OCT images lacked clarity in this region. Second, the study
360 defined stromal thickness as total corneal thickness minus epithelium thickness. Thus,
361 stromal thickness in our study included the Bowman membrane, Descemet membrane,
362 and endothelium, and these layers could not be separated in the image analysis.
363 Finally, variations in the follow-up time after commencing lens wear, due to booking
364 restrictions and participants' personal issues (34 ± 6 days, range: 27 - 43) may have
365 caused some variability in changes in thickness and radius of curvature.

366 In conclusion, this study introduced a new custom-built method to automatically detect
367 the anterior corneal surface, the epithelial posterior surface, and the posterior corneal
368 surface in OCT scans. Overnight wear of Ortho-K lenses caused thinning of the central
369 corneal epithelium. The anterior corneal surface became flattened while the anterior
370 and posterior surfaces of the stroma did not undergo significant changes. The
371 reduction in myopic refractive error caused by Ortho-K lens wear was mainly due to
372 changes in corneal epithelium thickness profile.

373 **Author contributions**

374 Conceptualization: Ahmed Abass, Ahmed Elsheikh.

375 provision of materials, patients or resources: Jun Jiang, FangJun Bao, Fan Jiang.

376 Data curation: Ashkan Eliasy, Bernardo T. Lopes.

377 Code: Ziyang Ran, Ahmed Abass.

378 Formal analysis: Ziyang Ran, Joshua Moore.

379 Methodology: Ahmed Abass, Ahmed Elsheikh.

380 Project administration: Ahmed Elsheikh, Ahmed Abass.

381 Supervision: Ahmed Elsheikh, Ahmed Abass.

382 Validation: Ashkan Eliasy, Bernardo T. Lopes.

383 Visualization: Ziyang Ran.

384 Writing - original draft: Ziying Ran, Hongmei Guo, Fan Jiang, Ahmed Abass
385 Writing - review & editing: Ziying Ran, Fan Jiang, Joshua Moore, Ahmed Abass,
386 Ahmed Elsheikh.

387 All authors read and approved the final manuscript.

388 **Funding**

389 This research received no specific grant from any funding agency in the public,
390 commercial, or not-for-profit sectors.

391 **Ethics**

392 This prospective study was approved by the Ethics Committee of the Eye Hospital of
393 Wenzhou Medical University. The ethical approval number is KYK [2015] 29. The
394 inclusion criteria were as follows: 8 to 18 years of age, spherical equivalent from -1.00
395 D to -6.00 D, best-corrected visual acuity greater than 20/25, intraocular pressures
396 were within normal limits (11~21mmHg), no history of Ortho-K lens wearing, no contact
397 lens contraindications or related eye and systemic disease. Patients who had
398 uncorrected visual acuity less than 20/25 or unacceptable lens decentration after
399 regular wear for one month had been excluded from the study. All procedures
400 complied with the Declaration of Helsinki. All the examinations were conducted after
401 the participants and their guardians fully understood and signed informed consent.

402 **Competing interests**

403 We declare we have no competing interests.

404

405 **Reference**

- 406 1. Holden BA, Fricke TR, Wilson DA, Jong M, Naidoo KS, Sankaridurg P, et al. Global prevalence
407 of myopia and high myopia and temporal trends from 2000 through 2050. *Ophthalmology*.
408 2016;123(5):1036-42.
- 409 2. Swarbrick HA. Orthokeratology review and update. *Clinical and Experimental Optometry*.
410 2006;89(3):124-43.
- 411 3. Bullimore MA, Johnson LA. Overnight orthokeratology. *Contact Lens and Anterior Eye*.
412 2020;43(4):322-32.
- 413 4. Mountford J. An analysis of the changes in corneal shape and refractive error induced by
414 accelerated orthokeratology. *International Contact Lens Clinic*. 1997;24(4):128-44.
- 415 5. Caroline PJ. Contemporary orthokeratology. *Contact Lens & Anterior Eye*. 2001;24(1):41-6.
- 416 6. Nichols JJ, Marsich MM, Nguyen M, Barr JT, Bullimore MA. Overnight orthokeratology.
417 *Optometry and Vision Science*. 2000;77(5):252-9.

- 418 7. Charm J, Cho P. High myopia-partial reduction ortho-k: a 2-year randomized study.
419 Optometry and Vision Science. 2013;90(6):530-9.
- 420 8. Kakita T, Hiraoka T, Oshika T. Influence of overnight orthokeratology on axial elongation in
421 childhood myopia. Investigative Ophthalmology & Visual Science. 2011;52(5):2170-4.
- 422 9. Wang J, Fonn D, Simpson TL, Sorbara L, Kort R, Jones L. Topographical thickness of the
423 epithelium and total cornea after overnight wear of reverse-geometry rigid contact lenses for
424 myopia reduction. Investigative Ophthalmology & Visual Science. 2003;44(11):4742-6.
- 425 10. Chen R, Mao X, Jiang J, Shen M, Lian Y, Zhang B, et al. The relationship between corneal
426 biomechanics and anterior segment parameters in the early stage of orthokeratology: a pilot study.
427 Medicine (Baltimore). 2017;96(19):e6907.
- 428 11. Lian Y, Shen M, Jiang J, Mao X, Lu P, Zhu D, et al. Vertical and horizontal thickness profiles of
429 the corneal epithelium and Bowman's layer after orthokeratology. Investigative Ophthalmology &
430 Visual Science. 2013;54(1):691-6.
- 431 12. Alharbi A, Swarbrick HA. The effects of overnight orthokeratology lens wear on corneal
432 thickness. Investigative Ophthalmology & Visual Science. 2003;44(6):2518-23.
- 433 13. Gifford P, Au V, Hon B, Siu A, Xu P, Swarbrick HA. Mechanism for corneal reshaping in
434 hyperopic orthokeratology. Optometry and Vision Science. 2009;86(4):e306–e11.
- 435 14. Li X, Friedman IB, Medow NB, Zhang C. Update on orthokeratology in managing progressive
436 myopia in children: efficacy, mechanisms, and concerns. Journal of Pediatric Ophthalmology &
437 Strabismus. 2017;54(3):142-8.
- 438 15. Zhang J, Li J, Li X, Li F, Wang T. Redistribution of the corneal epithelium after overnight wear
439 of orthokeratology contact lenses for myopia reduction. Contact Lens & Anterior Eye.
440 2020;43(3):232-7.
- 441 16. Kim WK, Kim BJ, Ryu IH, Kim JK, Kim SW. Corneal epithelial and stromal thickness changes in
442 myopic orthokeratology and their relationship with refractive change. PLoS One.
443 2018;13(9):e0203652.
- 444 17. Ambrósio R, Jr., Valbon BF, Faria-Correia F, Ramos I, Luz A. Scheimpflug imaging for laser
445 refractive surgery. Current Opinion in Ophthalmology. 2013;24(4):310-20.
- 446 18. de Sanctis U, Missolungi A, Mutani B, Richiardi L, Grignolo FM. Reproducibility and
447 repeatability of central corneal thickness measurement in keratoconus using the rotating
448 Scheimpflug camera and ultrasound pachymetry. American Journal of Ophthalmology.
449 2007;144(5):712-8.
- 450 19. Gonzalez-Mesa A, Villa-Collar C, Lorente-Velazquez A, Nieto-Bona A. Anterior segment
451 changes produced in response to long-term overnight orthokeratology. Current Eye Research.
452 2013;38(8):862-70.
- 453 20. Hrynchak P, Simpson T. Optical coherence tomography: an introduction to the technique
454 and its use. Optometry and Vision Science. 2000;77(7):347-56.
- 455 21. Ma Y, He X, Zhu X, Lu L, Zhu J, Zou H. Corneal epithelium thickness profile in 614 normal
456 chinese children aged 7-15 years old. Scientific Reports. 2016;6:23482.
- 457 22. Werkmeister RM, Sapeta S, Schmidl D, Garhofer G, Schmidinger G, Aranha Dos Santos V, et
458 al. Ultrahigh-resolution OCT imaging of the human cornea. Biomedical Optics Express.
459 2017;8(2):1221-39.
- 460 23. Nieto-Bona A, Gonzalez-Mesa A, Nieto-Bona MP, Villa-Collar C, Lorente-Velazquez A. Long-
461 term changes in corneal morphology induced by overnight orthokeratology. Current Eye Research.
462 2011;36(10):895-904.
- 463 24. Haque S, Fonn D, Simpson T, Jones L. Corneal and epithelial thickness changes after 4 weeks
464 of overnight corneal refractive therapy lens wear, measured with optical coherence tomography.
465 Eye Contact Lens. 2004;30(4):189-93; discussion 205-6.
- 466 25. Elsayy A, Abdel-Mottaleb M, Sayed IO, Wen D, Roongpoovapatr V, Eleiwa T, et al. Automatic
467 segmentation of corneal microlayers on optical coherence tomography images. Translational Vision
468 Science & Technology. 2019;8(3):39.

- 469 26. Eichel JA, Bizheva KK, Clausi DA, Fieguth PW, editors. Automated 3D Reconstruction and
470 Segmentation from Optical Coherence Tomography 2010; Berlin, Heidelberg.
- 471 27. Jiang F, Huang X, Xia H, Wang B, Lu F, Zhang B, et al. The spatial distribution of relative
472 corneal refractive power shift and axial growth in myopic children: orthokeratology versus multifocal
473 contact lens. *Frontiers in Neuroscience*. 2021;15(690):686932.
- 474 28. Yu Lh, Jin Wq, Mao Xj, Jiang J. Effect of orthokeratology on axial length elongation in
475 moderate myopic and fellow high myopic eyes of children. *Clinical and Experimental Optometry*.
476 2021;104(1):22-7.
- 477 29. Moore J, Shu X, Lopes BT, Wu R, Abass A. Limbus misrepresentation in parametric eye
478 models. *PLoS One*. 2020;15(9):e0236096.
- 479 30. Dubbelman M, Sicam VA, Van der Heijde GL. The shape of the anterior and posterior surface
480 of the aging human cornea. *Vision Research*. 2006;46(6-7):993-1001.
- 481 31. Doughty MJ, Zaman ML. Human corneal thickness and its impact on intraocular pressure
482 measures: a review and meta-analysis approach. *Survey of Ophthalmology*. 2000;44(5):367-408.
- 483 32. Reinstein DZ, Gobbe M, Archer TJ, Couch D, Bloom B. Epithelial, stromal, and corneal
484 pachymetry changes during orthokeratology. *Optometry and Vision Science*. 2009;86(8):E1006-14.
- 485 33. Cheah PS, Norhani M, Bariah MA, Myint M, Lye MS, Azian AL. Histomorphometric profile of
486 the corneal response to short-term reverse-geometry orthokeratology lens wear in primate corneas:
487 a pilot study. *Cornea*. 2008;27(4):461-70.
- 488 34. Maseedupally V, Gifford P, Lum E, Swarbrick H. Central and paracentral corneal curvature
489 changes during orthokeratology. *Optometry and Vision Science*. 2013;90(11):1249-58.
- 490 35. Queiros A, Lopes-Ferreira D, Yeoh B, Issacs S, Amorim-De-Sousa A, Villa-Collar C, et al.
491 Refractive, biometric and corneal topographic parameter changes during 12 months of
492 orthokeratology. *Clinical and Experimental Optometry*. 2020;103(4):454-62.
- 493 36. Yoon JH, Swarbrick HA. Posterior corneal shape changes in myopic overnight
494 orthokeratology. *Optometry and Vision Science*. 2013;90(3):196-204.
- 495 37. Chen D, Lam AK, Cho P. Posterior corneal curvature change and recovery after 6 months of
496 overnight orthokeratology treatment. *Ophthalmic and Physiological Optics*. 2010;30(3):274-80.
- 497 38. Mathai TS, Lathrop KL, Galeotti J, editors. Learning To Segment Corneal Tissue Interfaces In
498 Oct Images. *IEEE 16th International Symposium on Biomedical Imaging 2019*.
- 499 39. Ortiz S, Pérez-Merino P, Alejandro N, Gamba E, Jimenez-Alfaro I, Marcos S. Quantitative
500 OCT-based corneal topography in keratoconus with intracorneal ring segments. *Biomedical Optics*
501 *Express*. 2012;3(5):814-24.

502

503